Hindawi
International Journal of Chemical Engineering
Volume 2021, Article ID 6681796, 9 pages
https://doi.org/10.1155/2021/6681796

Research Article

Alumina Support for Cobalt Catalyst in a Methane Dry Reforming Reaction: The Role of Water Content in a Solvent Medium

My Hien Thi Bach,[1] Ngoc Thang Tran,[1] Thanh Nha Thi Tran,[1] Van Cuong Nguyen,[1] and Hong Anh Thi Nguyen[2]

[1]*Faculty of Chemical Engineering, Industrial University of Ho Chi Minh City, 12 Nguyen Van Bao St, Go Vap, Ho Chi Minh 70000, Vietnam*
[2]*Faculty of Chemical Engineering, Ho Chi Minh City University of Food Industry, 140 Le Trong Tan St, Ho Chi Minh 70000, Vietnam*

Correspondence should be addressed to Hong Anh Thi Nguyen; anhnth@hufi.edu.vn

Received 14 November 2020; Revised 20 January 2021; Accepted 23 January 2021; Published 11 February 2021

Academic Editor: Eshorame Samuel Sanni

This study aimed to synthesize alumina from an inorganic aluminum nitrate precursor in various binary solvent systems of ethanol and water using the sol-gel self-assembly (SSA) method, employing a triblock copolymer, pluronic P123, as the pore-directing agent. The resulting materials were implemented as a support for the cobalt (Co) catalyst in a methane dry reforming (MDR) reaction at 1073 K under 1 atm. Regardless of the water percentage used in the support synthesis, the methane dry reforming reaction over Co catalysts on alumina supports showed the negligible change in conversion during the 12 h reaction. Moreover, there was evidence of large quantities of amorphous carbon and graphitic carbon on the spent catalyst surface. However, the low oxidation temperature of these deposited carbons could help maintain the balance between the carbon formation and the carbon elimination processes on the catalyst surface during the reforming reaction, hence prolonging the lifetime of the catalyst. The high conversion of methane (CH_4) from 64.6% to 82.8% and carbon dioxide (CO_2) from 70.7% to 86.6% for the MDR reaction over the as-prepared alumina-supported Co catalyst demonstrated a significant improvement in catalyst production for the MDR reaction from the viewpoint of large-scale applications.

1. Introduction

The increase in the average temperature and climate change caused by greenhouse gases has become serious global issues. The human activities such as the burning of oil, coal, and gas, as well as deforestation, are associated with energy-related carbon dioxide (CO_2) emissions in the atmosphere. Therefore, in addition to the need to find new eco-energy sources, the use of mineral resources in an ecological and environmental approach is also a significant concern. Consequently, the methane dry reforming (MDR) method has emerged as a potential approach for producing syngas from CO_2 and methane (CH_4), which is a significant feedstock for downstream petrochemical processes [1–6]. Although this approach could have environmental and economic benefits, the catalyst limitations have impeded it from wide-ranging applications in large-scale industrial production.

Noble metals, such as rhodium (Rh), ruthenium (Ru), and platinum (Pt), have significant catalytic activity for the MDR process in terms of conversion and coking inhibition [7]. However, the unavailability and expensive cost of these catalysts are major drawbacks preventing their use in industrial applications. To date, cobalt- (Co-) based catalysts have garnered considerable attention since they possess comparable catalytic activity and higher stability against temperature variations in comparison to noble metals [8, 9]. Moreover, different metal oxides have been evaluated as the support for a Co-catalyzed MDR reaction, such as oxides of the alkaline Earth elements, including magnesium oxide

(MgO), calcium oxide (CaO) [8], ceric dioxide (CeO_2) [10], lanthanum dioxide (LaO_2) [11], strontium oxide (SrO) [12], aluminum oxide (Al_2O_3) [13–16], and Santa Barbara Amorphous-15 (SBA-15) [17–19]. Among of these materials, mesoporous alumina (MA) has been proven to be a potential support because of its availability. Recent contributions in heterogeneous catalysis regarding porous support and mesoporous structure materials have been widely used as catalyst supports since they can facilitate the dispersion of the catalysts and confine the active particles inside their matrix, preventing them from aggregating during the reaction [17, 19–21]. Mesoporous alumina support is one of the materials that has a high potential for being screened for the same effects in a MDR reaction.

Sol-gel self-assembly (SSA) is a common approach used for mesoporous Al_2O_3 production due to its easy, accessible, and reproducible characteristics in fabricating mesoporous structures [22]. Most SSA processes have been conducted by employing an organic salt precursor dispersed on a soft template dissolved in anhydrous ethanol (C_2H_5OH) [22, 23]. However, the toxicity and the high cost of organic salt and anhydrous (C_2H_5OH) ethanol have made them the most unlikely substances for this purpose. Thus, interest in using a less expensive and readily available inorganic aluminum precursor in large-scale applications is increasing. Additionally, the presence of water in the solvent has a significant influence on the pore structure of the resulting alumina materials [24], thus enabling intrapellet diffusion of the active nanoparticles in the porous framework [25]. To the best of our knowledge, only a few studies have investigated the combination of an inorganic aluminum precursor and a binary solvent mixture (C_2H_5OH in H_2O) for synthesis of alumina using the SSA method, to act as a support for a Co catalyst in an MDR reaction. Therefore, instead of using an organic salt precursor and anhydrous ethanol, the present study employed a combination of an inorganic aluminum precursor and a binary solvent mixture (C_2H_5OH in H_2O) for alumina synthesis using the SSA method. The performance of the Co catalyst on the as-prepared supports for the MDR reaction was evaluated to determine the amount of water needed in the solvent when preparing the support.

2. Materials and Methods

2.1. Chemicals. Aluminum nitrate $Al(NO_3)_3{\cdot}9H_2O$ (≥98%) and fuming hydrochloric acid (HCl) (37%) were purchased from Merck (Darmstadt, Germany). Pluronic® P-123 (MV = 5800) and cobalt (II) nitrate ($Co(NO_3)_2{\cdot}6H_2O$, 98%) were obtained from Sigma-Aldrich (St. Louis, Missouri, US). C_2H_5OH (99.9%) was obtained from VWR Chemicals (Darmstadt, Germany). All the reagents were used directly without any further purification. All the gases, including CH_4, CO_2, nitrogen (N_2), and hydrogen (H_2), were of analytical grade and provided by Air Products and Chemicals, Inc.

2.2. Catalyst Synthesis. Al_2O_3 was prepared by dissolving 0.98 g of P-123 in 14.6 ml of the C_2H_5OH-H_2O solvent mixture with the following proportions of water: 0%, 25%, 50%, and 75%. This solvent mixture was mixed at an ambient temperature for 30 min, followed by adding 3.68 g of $Al(NO_3)_3{\cdot}9H_2O$ and dropping 1.6 ml HCl (37%) solution. The obtained blend was additionally stirred for 60 min prior to undergoing the hydrothermal process at 373 K for 24 h in an autoclave. The obtained mixture was dried in the oven for 48 h at 333 K and then calcined in a furnace for 5 h at 1073 K.

The Al_2O_3-supported Co catalyst was prepared using the incipient wetness impregnation method. In particular, 0.28 g of the $Co(NO_3)_2{\cdot}6H_2O$ precursor was mixed with 0.25 ml of C_2H_5OH, and the resulting solution was sprayed on 0.5 g of as-synthesized alumina. The resulting mixture was dried overnight at 373 K and then calcined at 873 K for 5 h. The individual alumina support, prepared from the binary solvent system with a water content of 0%, 25%, 50% and 75%, was labelled as MA00, MA25, MA50, and MA75, respectively. Consequently, the supported Co catalysts synthesized from the abovementioned support were denoted as 10Co/MA00, 10Co/MA25, 10Co/MA50, and 10Co/MA75.

2.3. Catalyst Properties. The phases and crystalline structure of the selected spent catalysts were determined using a Rigaku Miniflex 600 X-ray diffraction instrument, which employed a copper (Cu) target as the radiation source at the wavelength of 1.5418 Å. The test specimen was scanned from 3° to 80° with the speed of $1^\circ\,\text{min}^{-1}$.

The amount of deposited carbons on the spent catalysts was quantified via the thermal programmed oxidation conducted on a TA TGA Q500 equipment (TA Instruments, Newcastle, DE, USA). In particular, the sample was heated at 373 K in N_2 atmosphere for 30 min to eliminate the volatile compounds, followed by increasing the temperature to 1023 K in a mixture flow of 20% O_2 in N_2 with a ramping rate of $10\,\text{K}\,\text{min}^{-1}$. The oxidation stage at 1023 K was left for an additional 30 min prior to cooling to room temperature.

The surface morphology of the selected catalysts was elucidated using scanning electron microscope (SEM) equipped with an energy-dispersive X-ray (EDX) detector (Hitachi Tabletop Microscope TM3030 Plus unit, Hitachi High Technologies Corp., Tokyo, Japan) and a Raman spectrometer employing 532 nm laser excitation (JASCO NRS-3100, Tokyo, Japan).

2.4. Catalytic Activity Evaluation. The fixed-bed reactor with a 3/8 diameter was used to evaluate the MDR reaction catalyzed by the alumina-supported Co at a fixed gas hourly space velocity (GHSV) of $36\,\text{L}{\cdot}\text{g}_{\text{cat}}{}^{-1}{\cdot}\text{h}^{-1}$. Prior to each assessment, H_2 reduction was done in situ at 1073 K for 1 h using a mixed flow of 50% H_2 in N_2. The output products were analyzed in an Agilent 6890 gas chromatography (Agilent Technologies, Santa Clara, CA, USA). The reactant conversions (X_i with i: CH_4 and CO_2) and product yields

(Y_{CO} and Y_{H_2}) were estimated using the following equations, respectively:

$$X_i(\%) = \frac{F_i^{in} - F_i^{out}}{F_i^{in}} \times 100\%, \quad (1)$$

$$Y_{CO}(\%) = \frac{F_{CO}^{out}}{\left(F_{CH_4}^{in} + F_{CO_2}^{in}\right)} \times 100\%, \quad (2)$$

$$Y_{H_2}(\%) = \frac{F_{H_2}^{out}}{2\,x\,F_{CH_4}^{in}} \times 100\%, \quad (3)$$

where F^{in} and F^{out} are the inlet and outlet molar flow rates (mol s^{-1}), respectively.

3. Results and Discussion

3.1. Catalyst Assessment of the MDR Reaction

3.1.1. Effect of Different Types of Alumina Support on the MDR Reaction. Four substrates, prepared using a mixed-solvent of C_2H_5OH and different proportions of H_2O (0%, 25%, 50%, or 75%), were applied as a support for the Co catalyst, and the catalytic performance of the substrates for the MDR reaction was evaluated at a stoichiometric feed ratio and temperature of 1073 K. As seen in Figures 1–4, the conversion of the reactants and the product yield were unchanged within the 12 h reaction, indicating the firm stability of the four catalysts under MDR reaction conditions. The conversion of CO_2 and CH_4 in the MDR reaction showed a decreasing trend from 86.6% to 70.7% and from 82.8% to 64.6%, respectively, in the order of 10Co/MA00 > 10Co/MA25 > 10Co/MA50 > 10Co/MA75 catalysts. This decrease in catalyst performance along with an increase in the water concentration in the solvent for the support preparation could be due to the modification in the support's pore structure, which was caused by the increase in the water content. Thus, the MDR reaction performance strongly depends on the support's features and the active Co metal properties, such as crystal size and dispersion [26]. Furthermore, it has been reported that the percentage of water in the solvent mixture has a significant impact on enlarging the pore diameter of MA produced using the SSA method [23], hence facilitating the generation of active metals with an appropriate size and enhancing the intrapellet diffusion of both the reactants and the products [25].

The effectiveness of the MDR reaction was consolidated via the time on stream (TOS) plot of the H_2 and CO formation yields, as seen in Figures 3 and 4. The support in catalyst activity was observed to play a significant role in both the CO and H_2 yields. In particular, the H_2 and CO yields were highest in the case of the 10% Co/MA00 catalyst; they were about 62.4–68.7% and 71.2–76.0%, respectively. When the MDR reaction was conducted with the 10% Co/MA75 catalyst, the CO yield decreased by approximately 10–20% and the H_2 yield decreased by approximately 20–30%. Regardless of the type of support, the H_2/CO ratio was always <1, thus proving the coexistence of the reverse water-gas-shift process in the MDR reaction [27].

3.1.2. Effect of CH_4 and CO_2 Partial Pressure on the MDR Reaction. To evaluate the partial pressure influence of CH_4 (P_{CH_4}) and CO_2 (P_{CO_2}) on MDR, the reactions over the 10% Co/MA00 catalyst were conducted with P_{CH_4} and P_{CO_2} in the range of 10–40 kPa at a temperature of 1023 K. Figure 5 shows the correlation between the CH_4 and CO_2 conversions with the change in P_{CH_4} at P_{CO_2} of 20 kPa (Figure 5(a)) and the change in P_{CO_2} at a fixed P_{CH_4} of 20 kPa (Figure 5(b)). The CH_4 conversion gradually decreased by approximately 15.0% as P_{CH_4} increased from 10 kPa to 40 kPa (see Figure 5(a)). This decrease in the CH_4 conversion was due to the upsurge in carbon formation caused by extreme CH_4 cracking in the surplus of the CH_4 feedstock. The formed carbon induced active sites blocking and hindering the catalytic performance of the MDR reaction [28]. In contrast, the CO_2 conversion increased and reached 80.6% when the P_{CH_4} increased from 10 kPa to 40 kPa.

Thus, the increase in P_{CH_4} resulted in superior CH_4 adsorption on the catalyst, therefore improving the CO_2 consumption through the MDR reaction [29]. A similar trend was also observed for the MDR reaction over the CeO_2-supported Co catalyst [28].

However, the CH_4 conversion showed continuous improvement to 82.7% when P_{CO_2} increased from 10 kPa to 40 kPa, while P_{CH_4} was kept at 20 kPa (see Figure 5(b)). This behaviour can be linked to the enhanced elimination of the deposited carbon, as depicted in equation (4) [30], and the coinciding existence of the CH_4 steam reforming process that was due to the increase in H_2O via the reverse water-gas-shift process, as follows [31]:

$$CH_4 \xrightarrow[-H_2]{} C_xH_{1-x} \xrightarrow[+CO_2]{} H_2 + CO \quad (4)$$

$$CO_2 + H_2 \leftrightarrow CO + H_2O \quad (5)$$

A decrease in the CO_2 conversion was found when P_{CO_2} increased from 10 kPa to 40 kPa (see Figure 5(b)), which could be due to the deficiency of CH_4 in reacting with the CO_2-rich feedstock. Furthermore, the presence of excess CO_2 in the reactor could intensify the possibility for active Co particles to be oxidized as follows, which resulted in a decrease in CO_2 adsorption [27]:

$$3Co + 4CO_2 \longrightarrow Co_3O_4 + 4CO \quad (6)$$

3.2. Characterization of the Spent Catalyst

3.2.1. XRD Analysis. The XRD spectrum of the synthesized 10% Co/MA00 after 12 h MDR reaction at 1073 K is shown in Figure 6. The peaks at 2θ of 37.6°, 45.6°, and 67.0° were assigned to the Al_2O_3 phase (JCPDS card no. 04-0858); the signals at 31.7°, 37.5°, and 44.6° corresponded to the Co_3O_4 crystalline phase (JCPDS card no. 74-2120). Moreover, the metallic Co presence was verified via the detection of a peak at 51.6° (JCPDS card no. 15-0806). The copresence of Co metallic and oxide particles in the 10% Co/MA00 sample indicated the occurrence of the redox cycle of the Co species during the MDR reaction. Notably, a broad peak at 2θ from

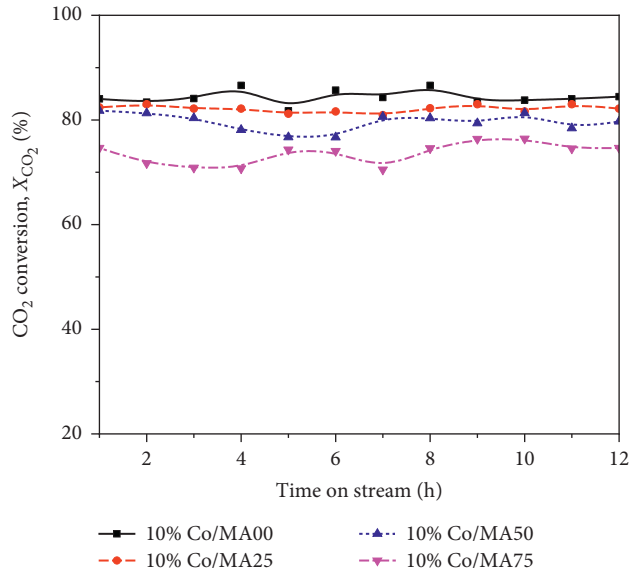

Figure 1: Time on stream conversion of CO_2 in MDR over different catalysts at 1073 K.

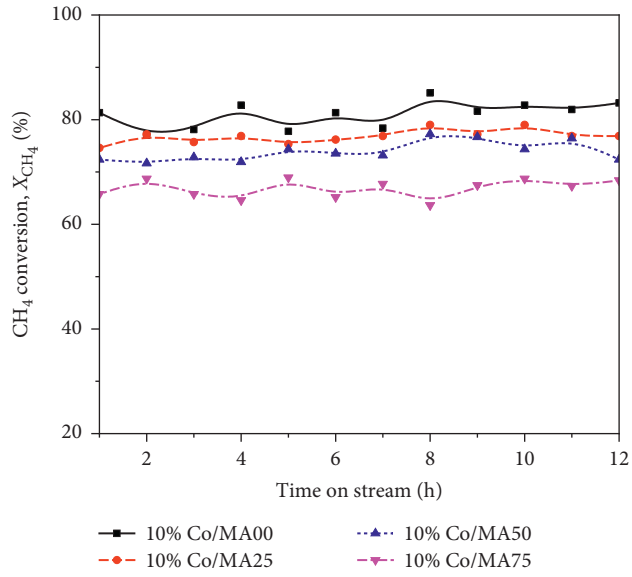

Figure 2: Time on stream conversion of CH_4 in MDR over different catalysts at 1073 K.

15.0° to 30.0° was deconvoluted into two separate diffraction signals, denoted as α and β, and displayed in a small inserted picture in Figure 6. The α peak represents amorphous carbon, and the β peak represents graphitic carbon [32].

3.2.2. Raman Measurements. Figure 7 shows the Raman spectrum of the 10% Co/MA00 after 12 h MDR reaction at 1073 K. Four active Raman peaks at 473.9 cm^{-1}, 517.7 cm^{-1}, 609.7 cm^{-1}, and 678.5 cm^{-1}, illustrated in the embedded picture, were assigned to the corresponding Co_3O_4 symmetric vibrational modes of E_g, F_{2g}, F_{2g}, and A_{1g}. The signal at 678.5 cm^{-1} represents the vibration of the octahedral site, and the E_g and F_{2g} modes are likely related to the mixed vibrations of the octahedral site and the tetrahedral oxygen movements [33]. These typical peaks were observed in the Raman spectra of the spent catalyst, suggesting that the reduced Co^0 species in the H_2 pretreatment were reoxidized to Co_3O_4 during the MDR reaction. Two peaks at 1338.5 cm^{-1} and 1573.5 cm^{-1} demonstrate the heterogeneity of the surface carbons including ordered carbon-like graphite (G-band) and amorphous carbon (D-band). The D-band was attributed to amorphous carbon or carbon nanofibers, while the G-band arises from the stretching of the C-C bond in graphitic carbon [34].

3.2.3. Surface Morphology Analyses. The SEM-EDX measurements of the 10% Co/MA00 catalyst after MDR at 1073 K suggest the presence of filamentous carbons or

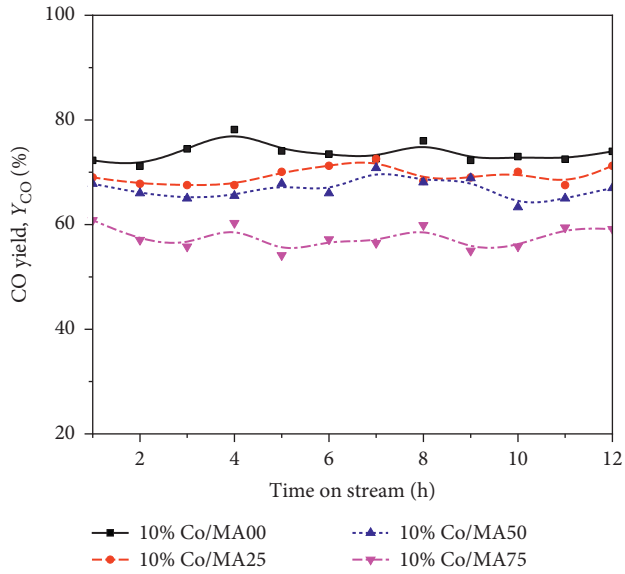

Figure 3: Time on stream yield of CO in MDR over different catalysts at 1073 K.

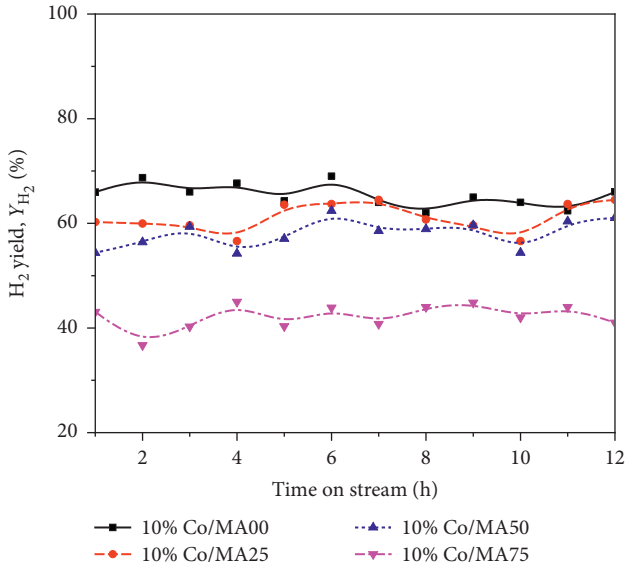

Figure 4: Time on stream yield of H_2 in MDR over different catalysts at 1073 K.

carbon fibers, as shown in Figure 8. The percentage of total carbon in the catalyst was around 64.03% based on the normalized EDX results. This could be due to the fact that the alumina-supported Co catalyst is known to boost the formation of filamentous carbon in a CH_4 atmosphere at high temperature [35].

3.2.4. TPO Measurements. Thermal-programmed oxidation (TPO) was performed to quantify the sum of the carbon deposits on the 10% Co/MA00 catalyst after MDR at 1073 K. As seen in Figure 9, about 77.1% weight of the sample was lost after the oxidation at temperatures ranging from 700 K to 850 K, which is in agreement with the EDX results (see Table 1). The differences in the results obtained from the two analytical methods could be due to the decomposition of the other elements in the TPO measurement.

Moreover, the low oxidation temperature of the deposited carbon at temperatures ranging from 750 K to 820 K, as determined from the derivative weight curves, suggest that all the deposits were well gasified in the reforming conditions; hence, they did not cause a loss of intrinsic catalyst activity or lengthen the lifetime of the catalyst [13].

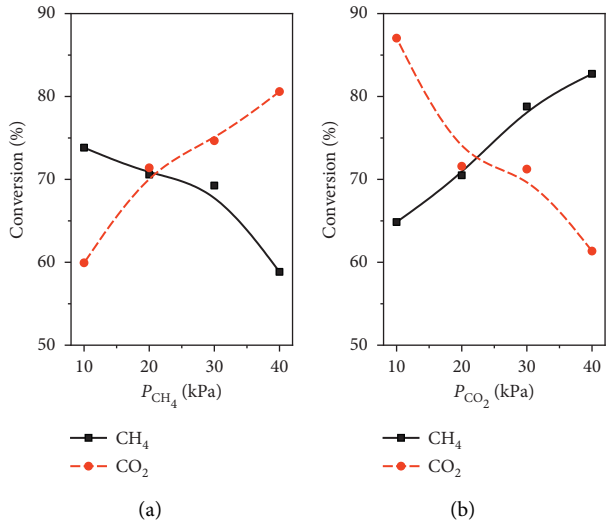

Figure 5: Influence of P_{CH_4} and P_{CO_2} on the CH_4 and CO_2 conversions in MDR over 10% Co/MA00 at 1023 K.

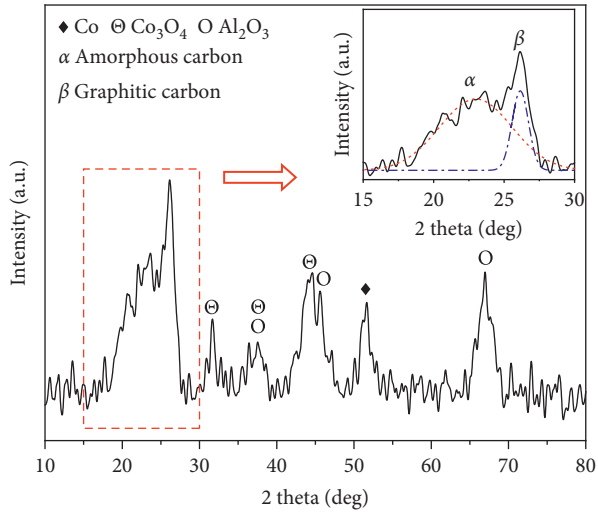

Figure 6: XRD spectra of spent 10% Co/MA00 after MDR at a stoichiometric feed ratio of 1 and 1073 K.

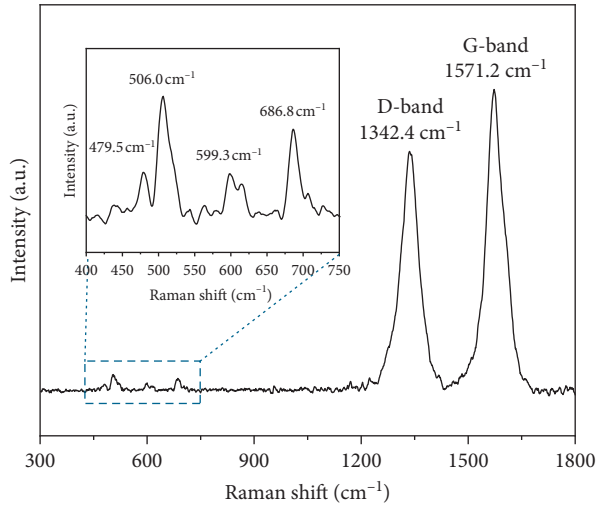

Figure 7: Raman spectra of the spent 10% Co/MA00 after MDR at 1073 K and stoichiometric feed ratio of 1.

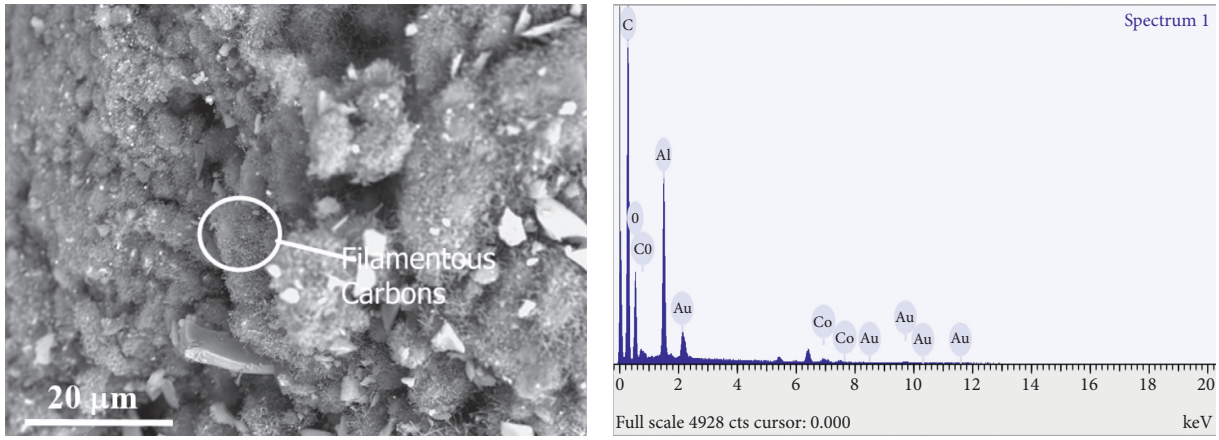

(a) (b)

Figure 8: (a) SEM image and (b) EDX analysis of the 10% Co/MA00 catalyst after MDR at 1073 K and a stoichiometric feed ratio of 1.

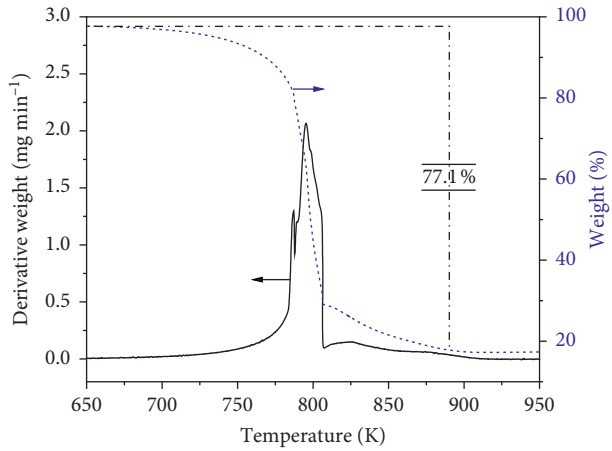

Figure 9: The weight loss and the derivative of weight loss profile of the 10% Co/MA00 catalyst after MDR at 1073 K and stoichiometric feed ratio of 1.

Table 1: EDX measurement of the 10% Co/MA00 catalyst after MDR at 1073 K.

Element	Weight (%)
Carbon (C)	64.03
Oxygen (O)	27.81
Aluminum (Al)	7.30
Cobalt (Co)	0.86

4. Conclusions

The performance of the Co catalysts supported on MA for the MDR reaction was investigated in terms of the support contribution. The water content in the solvent mixture applied for the Al_2O_3 support synthesis plays a crucial role in assembling the structure; hence, it influences the catalytic activity in the MDR reaction. Regardless of the type of support used, the Co catalysts showed good stability under 12 h MDR reaction. Notably, the 10% Co/MA00 catalyst demonstrated the highest activity for the MDR reaction with a carbon monoxide yield of 71.2–76.0%, and the deposit on the spent 10% Co/MA00 catalyst surface was found to consist of both amorphous carbon and graphitic carbon possessing low-oxidation temperature property and hence easily be eliminated in situ the reaction process. Moreover, the reactant partial pressure was found to have a significant impact on the CO_2 and CH_4 conversions as well as the product yields when the MDR reaction was conducted at 1023 K.

Data Availability

All experimental data used to support the findings of this study are available within the article.

Conflicts of Interest

The authors declare that they have no conflicts of interest.

Acknowledgments

The research was supported by the Industrial University of Ho Chi Minh City (no. 171.4081).

References

[1] O. R. Inderwildi, S. J. Jenkins, and D. A. King, "Mechanistic studies of hydrocarbon combustion and synthesis on noble metals," *Angewandte Chemie International Edition*, vol. 47, no. 28, pp. 5253–5255, 2008.

[2] L. Kapokova, S. Pavlova, R. Bunina et al., "Dry reforming of methane over $LnFe_{0.7}Ni_{0.3}O_{3-\delta}$ perovskites: influence of Ln nature," *Catalysis Today*, vol. 164, no. 1, pp. 227–233, 2011.

[3] M. Bradford and M. A. Vannice, "CO_2 reforming of CH_4," *Catalysis Reviews*, vol. 41, no. 1, pp. 1–42, 2007.

[4] M. Usman, W. M. A. Wan Daud, and H. F. Abbas, "Dry reforming of methane: influence of process parameters-a review," *Renewable and Sustainable Energy Reviews*, vol. 45, pp. 710–744, 2015.

[5] B. Abdullah, N. A. Abd Ghani, and D.-V. N. Vo, "Recent advances in dry reforming of methane over Ni-based catalysts," *Journal of Cleaner Production*, vol. 162, pp. 170–185, 2017.

[6] D.-V. N. Vo, T.-H. Nguyen, E. M. Kennedy, B. Z. Dlugogorski, and A. A. Adesina, "Fischer-Tropsch synthesis: effect of promoter type on alumina-supported Mo carbide catalysts," *Catalysis Today*, vol. 175, no. 1, pp. 450–459, 2011.

[7] S. Y. Foo, C. K. Cheng, T.-H. Nguyen, and A. A. Adesina, "Oxidative CO_2 reforming of methane on alumina-supported Co–Ni catalyst," *Industrial & Engineering Chemistry Research*, vol. 49, no. 21, pp. 10450–10458, 2010.

[8] E. Ruckenstein and H. Y. Wang, "Carbon dioxide reforming of methane to synthesis gas over supported cobalt catalysts," *Applied Catalysis A: General*, vol. 204, no. 2, pp. 257–263, 2000.

[9] A. W. Budiman, S.-H. Song, T.-S. Chang, C.-H. Shin, and M.-J. Choi, "Dry reforming of methane over cobalt catalysts: a literature review of catalyst development," *Catalysis Surveys from Asia*, vol. 16, no. 4, pp. 183–197, 2012.

[10] B. V. Ayodele, M. R. Khan, and C. K. Cheng, "Catalytic performance of ceria-supported cobalt catalyst for CO-rich hydrogen production from dry reforming of methane," *International Journal of Hydrogen Energy*, vol. 41, no. 1, pp. 198–207, 2016.

[11] B. V. Ayodele, M. R. Khan, S. S. Lam, and C. K. Cheng, "Production of CO-rich hydrogen from methane dry reforming over lanthania-supported cobalt catalyst: kinetic and mechanistic studies," *International Journal of Hydrogen Energy*, vol. 41, no. 8, pp. 4603–4615, 2016.

[12] K. Omata, N. Nukui, T. Hottai, Y. Showa, and M. Yamada, "Strontium carbonate supported cobalt catalyst for dry reforming of methane under pressure," *Catalysis Communications*, vol. 5, no. 12, pp. 755–758, 2004.

[13] É. Horváth, K. Baán, E. Varga et al., "Dry reforming of CH_4 on Co/Al_2O_3 catalysts reduced at different temperatures," *Catalysis Today*, vol. 281, pp. 233–240, 2017.

[14] S. Zeng, L. Zhang, X. Zhang, Y. Wang, H. Pan, and H. Su, "Modification effect of natural mixed rare earths on Co/γ-Al_2O_3 catalysts for CH_4/CO_2 reforming to synthesis gas," *International Journal of Hydrogen Energy*, vol. 37, no. 13, pp. 9994–10001, 2012.

[15] D. San-José-Alonso, J. Juan-Juan, M. J. Illán-Gómez, and M. C. Román-Martínez, "Ni, Co and bimetallic Ni–Co catalysts for the dry reforming of methane," *Applied Catalysis A: General*, vol. 371, no. 1-2, pp. 54–59, 2009.

[16] D. San José-Alonso, M. J. Illán-Gómez, and M. C. Román-Martínez, "Low metal content Co and Ni alumina supported catalysts for the CO_2 reforming of methane," *International Journal of Hydrogen Energy*, vol. 38, no. 5, pp. 2230–2239, 2013.

[17] J. Xin, H. Cui, Z. Cheng, and Z. Zhou, "Bimetallic Ni-Co/SBA-15 catalysts prepared by urea co-precipitation for dry reforming of methane," *Applied Catalysis A: General*, vol. 554, pp. 95–104, 2018.

[18] B. Erdogan, H. Arbag, and N. Yasyerli, "SBA-15 supported mesoporous Ni and Co catalysts with high coke resistance for dry reforming of methane," *International Journal of Hydrogen Energy*, vol. 43, no. 3, pp. 1396–1405, 2018.

[19] Z. Taherian, M. Yousefpour, M. Tajally, and B. Khoshandam, "Catalytic performance of Samaria-promoted Ni and Co/SBA-15 catalysts for dry reforming of methane," *International Journal of Hydrogen Energy*, vol. 42, no. 39, pp. 24811–24822, 2017.

[20] Q. Ma, J. Sun, X. Gao et al., "Ordered mesoporous alumina-supported bimetallic Pd-Ni catalysts for methane dry reforming reaction," *Catalysis Science & Technology*, vol. 6, no. 17, pp. 6542–6550, 2016.

[21] S. Singh, R. Kumar, H. D. Setiabudi, S. Nanda, and D.-V. N. Vo, "Advanced synthesis strategies of mesoporous SBA-15 supported catalysts for catalytic reforming applications: a state-of-the-art review," *Applied Catalysis A: General*, vol. 559, pp. 57–74, 2018.

[22] Q. Yuan, A.-X. Yin, C. Luo et al., "Facile synthesis for ordered mesoporous γ-aluminas with high thermal stability," *Journal of the American Chemical Society*, vol. 130, no. 11, pp. 3465–3472, 2008.

[23] W. Wu, Z. Wan, W. Chen, M. Zhu, and D. Zhang, "Synthesis of mesoporous alumina with tunable structural properties," *Microporous and Mesoporous Materials*, vol. 217, no. 15, pp. 12–20, 2015.

[24] W. Wu, M. Zhu, and D. Zhang, "The role of solvent preparation in soft template assisted synthesis of mesoporous alumina," *Microporous and Mesoporous Materials*, vol. 260, pp. 9–16, 2018.

[25] K. Tao, Y. Zhang, S. Terao et al., "Chemical and spatial promotional effects of bimodal pore catalysts for methane dry reforming," *Chemical Engineering Journal*, vol. 170, no. 1, pp. 258–263, 2011.

[26] A. L. M. Da Silva, J. P. Den Breejen, L. V. Mattos, J. H. Bitter, K. P. de Jong, and F. B. Noronha, "Cobalt particle size effects on catalytic performance for ethanol steam reforming-smaller is better," *Journal of Catalysis*, vol. 318, pp. 67–74, 2014.

[27] O. Omoregbe, H. T. Danh, C. Nguyen-Huy et al., "Syngas production from methane dry reforming over Ni/SBA-15 catalyst: effect of operating parameters," *International Journal of Hydrogen Energy*, vol. 42, no. 16, pp. 11283–11294, 2017.

[28] B. V. Ayodele, M. R. Khan, and C. K. Cheng, "Syngas production from CO_2 reforming of methane over ceria supported cobalt catalyst: effects of reactants partial pressure," *Journal of Natural Gas Science and Engineering*, vol. 27, pp. 1016–1023, 2015.

[29] M. A. Naeem, A. S. Al-Fatesh, W. U. Khan, A. E. Abasaeed, and A. H. Fakeeha, "Syngas production from dry reforming of methane over nano Ni polyol catalysts," *International Journal of Chemical Engineering and Applications*, vol. 4, no. 5, pp. 315–320, 2013.

[30] S. Y. Foo, C. K. Cheng, T. H. Nguyen, and A. A. Adesina, "Evaluation of lanthanide-group promoters on $Co–Ni/Al_2O_3$ catalysts for CH_4 dry reforming," *Journal of Molecular Catalysis A: Chemical*, vol. 344, no. 1-2, pp. 28–36, 2011.

[31] A. Donazzi, A. Beretta, G. Groppi, and P. Forzatti, "Catalytic partial oxidation of methane over a 4% Rh/α-Al_2O_3 catalyst part II: role of CO_2 reforming," *Journal of Catalysis*, vol. 255, no. 2, pp. 259–268, 2008.

[32] G. G. Tibbetts, G. L. Doll, D. W. Gorkiewicz et al., "Physical properties of vapor-grown carbon fibers," *Carbon*, vol. 31, no. 7, pp. 1039–1047, 1993.

[33] A. Diallo, A. C. Beye, T. B. Doyle, E. Park, and M. Maaza, "Green synthesis of Co_3O_4 nanoparticles via *Aspalathus linearis*: physical properties," *Green Chemistry Letters and Reviews*, vol. 8, no. 3-4, pp. 30–36, 2015.

[34] W.-W. Liu, S.-P. Chai, A. R. Mohamed, and U. Hashim, "Synthesis and characterization of graphene and carbon nanotubes: a review on the past and recent developments," *Journal of Industrial and Engineering Chemistry*, vol. 20, no. 4, pp. 1171–1185, 2014.

[35] F. Frusteri, G. Italiano, C. Espro, and F. Arena, "CH_4 decomposition on Ni and Co thin layer catalysts to produce H_2 for fuel cell," *Catalysis Today*, vol. 171, no. 1, pp. 60–66, 2011.